



Published in final edited form as:

*Neuron*. 2009 March 12; 61(5): 681–691. doi:10.1016/j.neuron.2009.01.026.

## Lesion Mapping of Cognitive Abilities Linked to Intelligence

Jan Gläscher<sup>1</sup>, Daniel Tranel<sup>3</sup>, Lynn K. Paul<sup>1</sup>, David Rudrauf<sup>3</sup>, Chris Rorden<sup>4</sup>, Amanda Hornaday<sup>3</sup>, Thomas Grabowski<sup>3</sup>, Hanna Damasio<sup>5,3</sup>, and Ralph Adolphs<sup>1,2,3</sup>

<sup>1</sup> Division of Humanities and Social Sciences, Caltech, Pasadena, CA

<sup>2</sup> Division of Biology, Caltech, Pasadena, CA

<sup>3</sup> Department of Neurology, University of Iowa, Iowa City, IA

<sup>4</sup> Department of Communication Sciences and Disorders, University of South Carolina, Columbia, SC

<sup>5</sup> Dornsife Cognitive Neuroscience Imaging Center, and Brain and Creativity Institute, University of Southern California, CA

### SUMMARY

The Wechsler Adult Intelligence Scale (WAIS) assesses a wide range of cognitive abilities and impairments. Factor analyses have documented four underlying indices that jointly comprise intelligence as assessed with the WAIS: verbal comprehension (VCI), perceptual organization (POI), working memory (WMI), and processing speed (PSI). We used non-parametric voxel-based lesion-symptom mapping in 241 patients with focal brain damage to investigate their neural underpinnings. Statistically significant lesion-deficit relationships were found in left inferior frontal cortex for VCI, in left frontal and parietal cortex for WMI, and in right parietal cortex for POI. There was no reliable single localization for PSI. Statistical power maps and cross-validation analyses quantified specificity and sensitivity of the index scores in predicting lesion locations. Our findings provide the most comprehensive lesion maps of intelligence factors to date, and make specific recommendations for interpretation and application of the WAIS to the study of intelligence in health and disease.

### Keywords

IQ; Wechsler Adult Intelligence Scale; Voxel-based Lesion Symptom Mapping; Language; Working Memory; Visuospatial Processing; Processing Speed; Verbal Comprehension

### INTRODUCTION

Studies of patients with focal brain damage have historically provided major insights into brain-cognition relationships, including Broca's famous case Tan (Broca, 1861) in regard to language, Phineas Gage in regard to social behavior (Damasio et al., 1994; Harlow, 1848), and H.M. in regard to memory (Scoville and Milner, 1957). While unique in the kinds of inference they permit, classical lesion studies are severely limited in their generalization and specificity because of typically small sample sizes (in the three examples cited: single cases) and large lesions. Group-level voxel-based lesion-symptom mapping (Bates et al., 2003; Damasio and

---

Address for correspondence: Ralph Adolphs, HSS 228-77, Caltech, Pasadena, CA 91125, radolphs@caltech.edu, (626)-395-4486.

**Publisher's Disclaimer:** This is a PDF file of an unedited manuscript that has been accepted for publication. As a service to our customers we are providing this early version of the manuscript. The manuscript will undergo copyediting, typesetting, and review of the resulting proof before it is published in its final citable form. Please note that during the production process errors may be discovered which could affect the content, and all legal disclaimers that apply to the journal pertain.

Frank, 1992) in large samples provides a powerful statistical tool to identify specific brain regions necessary for particular cognitive processes, and has become an indispensable comparison also for functional neuroimaging data. To date however, the application of lesion-symptom mapping has been rather limited to isolated cognitive domains including certain aspects of language (Dronkers et al., 2004), semantic knowledge (Damasio et al., 2004), emotion recognition (Adolphs et al., 2000), or spatial attention (Karnath et al., 2001), and other studies have typically not included comprehensive statistical analyses.

We used the Wechsler Adult Intelligence Scale (WAIS), a family of tests of cognitive domains contributing to intelligence created by David Wechsler (Wechsler, 1955, 1981, 1997), which is the single most widely used instrument for measuring intelligence today. Despite its construction as a test of cognitive aptitude, the WAIS is also ubiquitous in neuropsychological batteries that assess impairments (Rubin et al., 2005). It has excellent psychometric properties, very high test-retest reliability in both healthy (The Psychological Corporation, 1997) and clinical populations (Ryan and Cohen, 2003; Zhu et al., 2001), and an enormous database to provide comparison and standardization. Older, but still common, measures of cognitive domains derived from WAIS subtest scores are verbal IQ (VIQ), performance IQ (PIQ) and full-scale IQ (FSIQ). Verbal and performance IQ summarize abilities related to language and to visuospatial processing, respectively. More recent factor-analytic models of intelligence (Tulsky et al., 2003) and the advent of the latest version of the WAIS (the WAIS-III, Wechsler, 1997) produced four indices that define major cognitive domains: a verbal comprehension index (VCI), a perceptual organization index (POI), a processing speed index (PSI), and a working memory index (WMI) (The Psychological Corporation, 1997; Tulsky and Price, 2003) (see Table 2). Verbal comprehension and perceptual organization deficits have been broadly related to damage in left and right hemisphere respectively (Bornstein and Matarazzo, 1982; Warrington et al., 1986), and impairments in PSI, and to a lesser degree in WMI, have been reported following traumatic brain injury and multiple sclerosis (DeLuca et al., 2004; Fisher et al., 2000; Kennedy et al., 2003) which are commonly associated with a distributed pattern of lesions in many regions (Kido et al., 1992; Levine et al., 2005). Yet the detailed neuroanatomical underpinnings of these cognitive domains, and their sensitivity and specificity, remain largely unknown.

We used data available from 241 neurological patients with focal, chronic, stable brain lesions (see Table 1) who had been extensively characterized neuropsychologically and who were psychiatrically healthy. We mapped the locations of each patient's lesion (from CT or MR scans) manually onto a single reference brain (Damasio and Frank, 1992). Using voxel-based lesion-symptom mapping (Bates et al., 2003; Frank et al., 1997; Rorden et al., 2007) applied to the whole brain we mapped regions with significant lesion-deficit relationships using non-parametric tests with false-discovery rate corrections, a sophisticated statistical approach from modern neuroimaging. The results were compared to anatomical maps of statistical power (Rudrauf et al., 2008a). A cross-validation analysis using receiver operating characteristic (ROC) curves established the sensitivity and specificity shown by each of the four cognitive indices from the WAIS, revealing how well the index scores can predict lesions in specific brain regions. Additional analyses probed lesion maps for each of the four cognitive indices when all shared variance was removed, and explored possible differences in lesion maps as a function of gender and age.

## RESULTS

### Background Analyses

Background demographic variables (Table 1) showed some expected correlations with performance on the four cognitive indices we investigated; expectedly, all four correlated positively with years of education ( $p < 0.001$ ), and to some extent negatively with lesion volume

(the larger the lesion, the lower the score; see Supplementary Table 1). Although the distribution of lesions was inhomogeneous across the brain (Figure 1), statistical power maps confirmed that we had adequate power to detect effects in most regions, importantly including all regions where we in fact report findings (Supplementary Figure 1). Note that since the statistical power largely reflects the regional variations of vulnerability to brain injury, maximal power is observed in those brain regions that are most often clinically affected. Consistent with the primary etiologies (stroke, anterior temporal lobectomy resection due to intractable epilepsy; see Table 1), areas in the territory of the middle cerebral artery (MCA) and anterior temporal pole were sampled most densely (Figure 1).

The behavioral performance of our patient sample replicated the known 4-factor structure based on standardized WAIS-III index scores (The Psychological Corporation, 1997) (Supplementary Figure 2a). Because not all patients completed all subtests of the WAIS, and because some took different versions of the WAIS, we decided to run 2 factor analyses: (1) excluding the three subtests with the smallest sample sizes (matrix reasoning (n=84), letter-number sequencing (n=71), and symbol search (n=72)) yielding a sample size of n=117 (Supplementary Figure 2b), and (2) including only those patients who took all subtests (n=66) (Supplementary Figure 2c). Both approaches replicated the published factor structure based on healthy individuals, the first with a similarity coefficient  $R_V = 0.91$  ( $Z = 15.17$ ,  $p < 0.0001$ ) (Abdi, 2007), the second with  $R_V = 0.93$  ( $Z = 19.8$ ,  $p < 0.0001$ ). Thus our sample of lesion patients presented, as a group, a normal cognitive architecture, facilitating the interpretation of the following analysis of the relationship between the four cognitive indices and focal brain damage.

## Lesion Mapping

We first conducted voxel-based lesion-symptom mapping (VLSM) analyses based on full-scale IQ, verbal IQ, and performance IQ, the most common measures in clinical assessment. Lesions that impacted full-scale IQ overlapped primarily with those regions in which lesions also significantly affected verbal IQ, in particular in the left inferior frontal cortex, commonly involved in speech production (see Supplementary Figure 3). They were also found in the insular cortex, in fronto-polar cortex, and in parietal cortex and underlying white matter, which have also been implicated in volumetric studies of general intelligence (Colom et al., 2006a, b; Haier et al., 2004; Jung and Haier, 2007). This finding presumably reflects the verbal requirements of all WAIS subtests – at a minimum, subjects must understand verbally given instructions. As expected, verbal and performance IQ depended on regions in the left and right hemispheres, respectively. At a more detailed level, we found a reliance of verbal IQ on left frontal regions, commonly implicated in speech, whereas performance IQ relied on right parietal, occipital, and superior temporal regions, commonly implicated in visual and visuospatial processing. Full-scale, verbal, and performance IQ are often used for clinical assessment, but they stem from older versions of the WAIS and do not fully capture the results of modern factor analyses.

We therefore next analyzed the four cognitive indices provided by the WAIS-III. We first carried out an initial, neuroanatomically very coarse analysis that divided our patient sample into those with unilateral left and those with unilateral right hemisphere lesions. Since handedness would be expected to influence lateralization of processing, we tested the effects of lesion side and of handedness on the index scores in 4 separate ANOVAs. Of these, only the ANOVA for PSI revealed significant main effects (hemisphere:  $F=7.57$ ,  $p=0.007$ , handedness:  $F=4.86$ ,  $p=0.029$ ). It is possible that the null findings for all the other index scores are due to the small sample size of the left-handed patients (n=24 compared to 217 right-handed patients). The findings for PSI were further qualified by a significant interaction effect (hemisphere  $\times$  handedness:  $F=5.16$ ,  $p=0.024$ ; all other  $P_s > 0.05$ ) (see Supplementary Figure

4). This interaction effect in PSI was driven mainly by a difference in left-handed individuals whose PSI scores differed depending on the side of lesion (left hemi < right hemi). For PSI, the subsequent VLSM analyses described next were therefore initially conducted with left- and right-handed patients independently, but this did not reveal any significant differences in lesion localization between groups. Thus, for all subsequent analyses reported hereafter, left- and right-handed patients were combined. Our initial analysis reported above suggests that hemispheric side of lesion is likely too coarse an anatomical measure to yield much insight into the possible localization of intelligence factors. We turn next to the focus of our study, a VLSM analysis, which revealed a considerably more detailed localization of the lesion-deficit relationship (Figure 2). Significant effects for POI were found only in the right hemisphere covering a large part of the MCA territory and in temporo-occipito-parietal regions (Figure 2a). Specifically, maximum lesion-deficit relationship for POI was found in the supramarginal gyrus, the posterior part of the superior temporal sulcus (STS) (near the temporo-parietal junction, TPJ), the posterior inferior frontal gyrus (IFG), and the dorsal bank of the middle STS.

The locations of significant lesion-deficit relationships for VCI and WMI largely overlapped in the anterior aspects of the MCA territory in the left hemisphere, extending also posteriorly into the parietal lobule (Figure 2b and 2c). However, these index scores exhibited different peak locations for the maximum lesion-deficit relationship: the peak for VCI was located in pars opercularis and pars triangularis of the left inferior frontal cortex (Broca's area) and its underlying white matter, as well as in the left external capsule. By contrast, the maximum effect for WMI was found in the anterior and posterior bank of the central sulcus and the underlying white matter as well as in the postcentral gyrus. In addition, the white matter tracts underneath the precentral gyrus were also related to WMI deficits. Coordinates of these and other local peaks (in MNI space) are listed in Table 3.

Finally, PSI was associated with various clusters of voxels distributed across frontal and parietal regions in both hemispheres. Specifically, we found local peaks for lesion-deficit relationship for PSI in the left hemisphere in the anterior precentral gyrus, in the posterior bank of the postcentral sulcus, in inferior parietal gyrus and lingual gyrus; significant effects in the right hemisphere were located along the right middle frontal gyrus and in the right posterior IFG (Figure 2d).

To examine the findings that were entirely specific to a single cognitive factor, we also carried out an analysis that removed all variance shared in common among the four factors. The results retain the overall pattern but generally show considerable spatial restriction, due to the decreased statistical power resulting from reducing the performance variance (Supplementary Figure 5). Notably, the findings for VCI, the index with the most substantial shared variance, were limited to the left anterior temporal pole and the left caudate head. Possibly, this reflects the fact that the original lesion maps for VCI and WMI overlapped to a large degree in the left hemisphere (cf. Figure 2), and removing shared variance in performance resulted in removing the shared anatomical regions. This interpretation was supported by a further analysis, in which we residualized VCI and WMI only with respect to each other, but not with respect to POI and PSI (Supplementary Figure 6). Here we found that removing the variance of the other score is sufficient to essentially eliminate most significant lesion-deficit effects, especially in the inferior frontal cortex. These findings together with Figure 2 argue that VCI and WMI largely share a common neural substrate.

Given that the index scores are composites based on multiple subtests, how much variability in the neuroanatomical substrate exists between the different subtests contributing to a single index score? Relatedly, how representative are the lesion maps from a given subtest of the cognitive index to which it contributes? We addressed these questions by conducting the same

VLSM analyses for each and every subtest (Figure 3) and then calculating the amount of spatial overlap between the significant clusters in the individual subtest and the index score to which it contributes (Figure 4). This overlap measure can be calculated as the percentage of voxels of each subtest score that overlap with each index score (Figure 4A) or as the percentage of voxels of each index score that is overlapped by each subtest score (Figure 4B). Whereas the former measure is not biased by the extent of significant effects in the subtest scores, the latter reveals how representative a particular subtest score is for each index score.

With the exception of the Symbol Search subtest, which overlapped to a greater degree with POI than with the cognitive index to which it contributes (PSI), we found that the lesion maps associated with subtests were generally subsets of the lesion maps for their respective index scores (Figure 4A). Consistent with the overlapping localization of VCI and WMI in the left hemisphere, we also observed that the subtests of these index scores overlapped with the location of both of these index scores. Interestingly, the Digit Symbol/Coding subtest of the PSI also overlapped with locations of VCI and WMI, further evidence that the two subtests of the PSI really measure two different neuropsychological processes rather than a distinct single factor of PSI. Also surprising was the finding that while Digit Span was highly representative of the lesion pattern associated with its cognitive index, WMI (0.95), it overlapped only 68 % with WMI (compare cells in Figure 4A and 4B). Overall, the pattern of findings suggests that, at least to some degree, the subtests that comprise the cognitive indices each contribute to that index only to some extent; however, all subtests also contribute more or less to one or more of the other cognitive indices and retain a unique lesion location suggesting that they indeed reflect processes that are not captured by any of the four cognitive indices.

### Sensitivity and Specificity

To test for the sensitivity and specificity of each index score in predicting the lesion locations we found (Figure 2), we conducted a cross-validation analysis. We used a leave-one-out VLSM analysis for each patient and determined how much each patient's lesion overlaps with the rest of the sample. These data in combination with the index scores were used to derive the area under the receiver operating characteristic (ROC) curve. Using a permutation test we were able to statistically compare the performance of each index score in predicting a lesion in the brain area associated with that index score (Figure 2) and in those brain areas associated with each of the other index scores (for details, see Methods). Each index score significantly predicted a lesion in its associated brain area with the exception of PSI, thus demonstrating the sensitivity of POI, VCI, and WMI (see Figure 5). However, consistent with the large overlap in the lesion maps for VCI and WMI (Figure 2) these two indices also significantly predicted a lesion in the brain region associated with the other index; that is, these two indices were not very specific with respect to identifying separate lesion locations (Figure 5B and 5C). A much better specificity was found for POI (Figure 5A) which predicted lesions only within their focus in the right hemisphere. Finally, PSI significantly predicted lesion in both the left (WMI) and right (POI) hemisphere, suggesting that the specificity of this index score is questionable (Figure 5D) or that it is not reliably associated with a specific lesion location. In conclusion, this cross-validation analysis demonstrated that (i) POI is sensitive and specific for right hemispheric lesions with a focus in parieto-occipital and superior temporal cortex, (ii) VCI and WMI are sensitive and specific for left hemisphere lesions with a focus in frontoparietal cortex, but do not discriminate between the lesion loci associated with these two indices, and (iii) that PSI is neither sensitive nor specific for predicting lesions in the brain areas revealed in the initial VLSM analysis.

### Effects of Gender and Age

A final and more exploratory set of analyses examined whether there might be different lesion maps for the four cognitive indices for males as compared to females, or for young as compared

to old patients. Recent studies have highlighted gender (Haier et al., 2005; Jung et al., 2005) as well as age differences (Haier et al., 2004) related to general intelligence (as estimated with FSIQ) using both volumetric measures of gray and white matter as well as markers of intracellular metabolites. These studies showed that whereas males show stronger correlations between gray matter and FSIQ in superior frontal (BA 8, 9) and in temporo-parietal regions (BA 39, 40), significant correlations for females occur in inferior frontal cortex (BA 10) including Broca's area (Haier et al. 2005). Likewise, stronger correlations were found between gray matter and FSIQ in the medial PFC, whereas for older subjects the peak was in the lateral PFC (Haier et al., 2004).

In contrast to these studies that investigated FSIQ, our approach was targeted at domain-specific intelligence factors embodied in the WAIS index scores. To explore effects of gender and age, we conducted separate ANOVAs to explore the effects of age, gender, and lesion size, including these as three factors and including all their interactions. For VCI and WMI, lesion size was the single significant factor (both  $F_s > 3.71$ , both  $P_s < 0.03$ ) and none of the interactions were significant, arguing that the effect of having a lesion, and its extent, swamp any effects of gender or age. PSI and POI failed to show any significant effects at all in this analysis.

Despite the lack of any significant effect of age or gender in the above ANOVAs, we generated exploratory lesion maps for each gender, and for young and old subjects. It should be emphasized that these analyses are meant only to be exploratory at this stage, since they are limited to our particular sample and since there are systematic effects of gender and age on lesion distribution (irrespective of performance on the WAIS). We found stronger effects for women with left hemisphere lesions on all index scores (including inferior frontal areas as in Haier et al., (2005), whereas men had stronger lesion-deficit relationships for POI and PSI in the right, and for VCI and WMI in the left hemisphere (Supplementary Figure 7). In addition, we found stronger lesion deficit relationship for young patients on POI in the right hemisphere, whereas for VCI and WMI both age groups overlapped in the left hemisphere with larger significant clusters for the older sample (Supplementary Figure 8). However, due to an inhomogenous distribution of lesions as a function of gender or age, the effects of these covariates on the neural substrate of intellectual abilities may be better investigated using neuroimaging in healthy individuals.

## DISCUSSION

We used non-parametric voxel-based lesion symptom mapping (VLSM) to detect lesion-deficit relationships in each of the four index scores derived from the WAIS as well as the subtests they comprise. Our large sample of patients with focal brain damage provided adequate statistical power over most of the brain at a relatively conservative, false-discovery rate corrected, threshold of 1%. We found that (i) impairments in VCI were associated with damage in left hemisphere, in particular in the left inferior frontal cortex, (ii) impairments in POI were associated with damage in right parietal, occipito-parietal and superior temporal cortex, (iii) impairments in WMI were associated with left hemispheric lesions particularly focused in superior parietal cortex, and (iv) impairments in PSI correlated with a number of small regions distributed across both hemispheres. These quantitative results at a comparatively high spatial resolution and statistical power provide a comprehensive set of lesion maps for each cognitive index.

Several novel insights emerged from these findings and the follow-up analyses we conducted. At the level of the four cognitive indices, we found that VCI and WMI share a common anatomical substrate that accounts for essentially all of their shared variance in behavioral performance. By contrast, PSI fragmented into two distinct anatomical substrates that depended on sectors in left and right hemisphere, and that corresponded to the two subtests comprising

the PSI. At the level of the individual subtests, there was a considerable range in how well their lesion maps represented the lesion map of their respective cognitive index, although in general these were subsets of each other. Finally, the power of each cognitive index score to predict lesion location varied in terms of sensitivity and specificity, with POI being the most powerful and PSI the least.

Our findings provide not only substantial new neuroanatomical detail, but also run counter to some prior studies. In one of the first meta-analyses on this topic, Bornstein and Matarazzo (Bornstein and Matarazzo, 1982) found evidence for an association of deficits in verbal IQ with left hemisphere lesions, and deficits in performance IQ with right hemisphere lesions. The latter finding was further refined by a lesion study that showed deficits mainly resulted from damage to the right parietal cortex (Warrington et al., 1986). Our findings for POI are consistent with these early accounts in gist, but provide considerably more detail and quantification. With respect to VCI, it is curious that we observed the most significant effects only in the left inferior frontal cortex (Broca's area), but not in the posterior superior temporal gyrus (Wernicke's area) and sulcus. By contrast, Bates et al. (2003), using patients with chronic aphasia, found a significant relationship between lesions in the posterior superior temporal gyrus and sulcus and a task of verbal comprehension, the Western Aphasia Battery. One possible reason for the discrepancy between our study and theirs may lie in the exclusion of severely aphasic patients in our study (the WAIS is not generally administered to very aphasic patients, since they would have difficulty understanding the task instructions), whereas Bates et al. (2003) specifically selected aphasic patients. In a follow-up analysis, we further probed this interpretation by comparing the VCI scores of patients with a lesion in Wernicke's area with the rest of the sample and found no significant difference between these groups ( $T_{225}=0.64$ ,  $p>0.5$ , see Supplementary Analyses for details).

A second possibility for the discrepancy between our studies and that of Bates et al. (2003) may be that the VCI, unlike the Western Aphasia Battery, is simply not a sensitive measure of verbal comprehension as it specifically relates to aphasia. We obtained some support for this idea by comparing our lesion map for the VCI with the lesion map for another test specifically of verbal comprehension, the Token Test, widely considered a sensitive neuropsychological test for Wernicke's aphasia (De Renzi and Vignolo, 1962). We analyzed the data of 141 patients from our original sample who had been given both the WAIS and the Token Test. The results for VCI on this subsample of patients are similar to our findings for the full sample and show lesion deficit relationships in the inferior frontal gyrus (Broca's area). However, the Token Test reveals a significant lesion effect additionally in the TPJ (Wernicke's area) and in the posterior STS and middle temporal gyrus (see Supplementary Figure 9). This comparison of the VCI with a test known to be sensitive to Wernicke's aphasia, in the same sample of patients, provides strong support for the idea that the Verbal Comprehension Index, despite its name, is less a measure of verbal comprehension *per se* and instead may tap a more abstract dimension related to verbal intelligence.

The neural correlates of working memory are commonly assessed in modern neuroscience using an *n*-back task (subjects are asked to compare the *n*-th previous item with the current item), a human analogue of the delayed match-to-sample task typically used to assess working memory in other species. In functional imaging studies, the *n*-back task very consistently activates a fronto-parietal network in both hemispheres, including dorsolateral and ventrolateral prefrontal cortex, dorsal cingulate, medial and lateral premotor cortex, and medial and lateral posterior parietal cortex (Owen et al., 2005). In contrast, our findings suggest a dominance of a left-lateralized network on WMI performance, a difference that may be due to a difference in sensitivity between lesion and activation studies. Another parsimonious explanation for the difference between our findings and those from neuroimaging studies of *n*-back tasks relates to the different kinds of responses typically required of subjects. Unlike

the *n*-back tasks, which can utilize a manual response (button-press) regardless of the verbal or nonverbal nature of the stimuli, the WMI subtests all require verbal responses. Lesions in the left posterior parietal cortex give rise to conduction aphasia which is – among other symptoms – characterized by a deficit in verbal repetition (Smith and Jonides, 1998), essentially manifesting as an impairment in verbal working memory. Thus, our lateralized findings for WMI may reflect the necessary circuitry for verbal working memory as opposed to the entire range of areas activated in functional imaging studies of working memory. Also, it is possible that the appearance of general deficits in working memory could require bilateral parietal lesions (our sample only included patients with a single lesion).

Our cross-validation analysis implied sensitivity and specificity for POI to predict right hemispheric lesions with a focus in the temporo-parietal area, and for VCI and WMI to predict left hemispheric lesion. However, PSI was not found to provide sufficient sensitivity and specificity to predict lesions in the many bilateral areas that showed a significant lesion-deficit relationship in the VLSM analysis (Figure 2). This lack of sensitivity and specificity is consistent with a common observation in neuropsychological diagnosis which suggests that lesions of heterogeneous etiology and location can result in impairments in processing speed (DeLuca et al., 2004; Kennedy et al., 2003; van der Heijden and Donders, 2003). However, processing speed might be in essence a test of the efficiency of inter-regional interactions in complex tasks, perhaps especially when they are distributed between the two hemispheres (Ringo et al., 1994).

In line with this idea, the VLSM analyses of the 2 subtests comprising PSI point to neuroanatomical correlates in different hemispheres (Figure 3), contributing to the heterogeneous pattern of lesion-deficit relationship for PSI (Figure 2). Digit Symbol/Coding was related primarily to left-hemisphere lesions in the frontal and parietal lobes and the underlying white matter. Consistent with this finding, a recent study found significant correlations between performance on the Digit Symbol test and fractional anisotropy (an index of fiber tract integrity) in left frontal, bilateral temporal, and parietal white matter. This suggests that the ability of these regions to communicate with others might have an influence on processing speed (Turken et al., 2008). In contrast, in our study symbol search was lateralized to the right hemisphere, consistent with its greater emphasis on spatial skills. Taken together, both studies suggest that communication between distributed brain areas, and perhaps especially ones distributed across the hemispheres, contributes to PSI performance.

The findings of this study have significant implications for neurological interpretations based on neuropsychological assessment. Perhaps most interesting from a clinical perspective are our results regarding the sensitivity and specificity of the WAIS indices in predicting lesion location. As expected, impaired POI scores are very likely to reflect damage in the parietal and/or occipital and temporal lobes of the right hemisphere. Although this encompasses a relatively large territory, it is uniquely related to POI. In contrast, the lesion sites responsible for WMI and VCI impairments overlap within the left hemisphere, even though these indices emerge as distinct dimensions in a factor analyses (Supplementary Figure 2) and have traditionally been associated with distinct psychological constructs. This finding suggests that a common neuro-cognitive factor may be underlying verbal comprehension and working memory as measured by the WAIS and may be critical for normal performance levels on both scores. Given the commonalities of the subtests comprising VCI and WMI, this common factor is most likely of verbal nature.

It is also worth reiterating that our patient sample comprised only subjects with a single lesion in the chronic epoch (>3 months post lesion onset) and thus is not suited to allow inferences regarding the effects of, or recovery from, acute lesions. Performance in chronic lesion patients is of course subject to reorganization and recovery, qualifying the inferences that can be drawn



about normal brain function (Ungerleider and Haxby, 1994). On the other hand, identifying a lesion-deficit relationship in the chronic epoch reveals brain regions that are critical and necessary in implementing a cognitive function in the sense that after damage to these areas the function never fully recovers (Rafal, 2006). This feature, together with the much more stable and often specific effects of the lesion on cognition, have long made the chronic epoch the time period of choice in our laboratory. Lesion studies continue to provide a powerful method for detecting brain regions necessary for a specific cognitive function, but because of the reliance on naturally occurring lesions they are also limited in that they do not sample each region equally. Functional neuroimaging studies are not subject to the same sampling pitfall as they can acquire whole-brain functional datasets, but they are fundamentally limited by the kinds of brain-behavior inferences possible, highlighting sufficient (but not necessary) brain regions (Price et al., 1999). Our study is distinguished by an unusually large number of patients with lesions sampling most of the brain (Figure 1), which together with quantitative statistical power maps (Supplementary Figure 1), greatly reduce the problem of potential false-negative findings.

Our findings complement a growing body of literature on the neural correlates of general intelligence that has used a variety of functional imaging approaches as well as lesions (Colom et al., 2006a, b; Duncan et al., 2000; Gray et al., 2003; Haier et al., 2004, 2005; Jung et al., 2005). While early accounts emphasized frontal cortex as the only site for general intelligence (Duncan et al., 2000), a recent comprehensive review of the field also implicated parietal, temporal and occipital cortex (Jung and Haier, 2007). The authors of this review argue for a distinction between “intelligence in general” (as measured by comprehensive summary scores such as full-scale IQ) and “general intelligence”, which they and others (Jensen, 1998) define as a “distillate of the common source of individual differences in all mental tests, completely stripped of their distinctive features of information content, skill, strategy, and the like.” The focus of our study was more on domain-specific intellectual faculties than on the neural architecture of general intelligence. Indeed, our data do not show evidence for a neural substrate that is shared among all WAIS subtests. It may be that the neural correlates of general intelligence are to be found in brain regions that maintain anatomical and functional connectivity with some or all of the areas implicated in the lesion-deficit maps of the individual subtests.

We also emphasize that the abilities measured by the WAIS and its derived index scores are by no means a comprehensive assessment of all human cognitive capacities. There are many other aspects of human mental life that also deserve to be counted as “intelligence” in addition to those capacities measured by the WAIS and similar batteries (Sternberg, 2000), notably those related to social and emotional functioning (Bar-On et al., 2003). Finally, we stress that our findings reveal only essential regions involved in cognition, not the entire network of structures that participate. Knowledge of the entire network, the contributions made by each of the components, and the role of white matter communication between them, will ultimately be required in order to understand how cognitive processes are implemented by the brain at systems level. That understanding will need to draw not only on lesion studies focusing on regions of the cerebral cortex such as the present one, but also on subcortical structures, white matter connectivity (Rudrauf et al., 2008b), and the functional effects that a lesion has on distal target structures (Price and Friston, 2002).

## EXPERIMENTAL PROCEDURES

### Subjects

The WAIS-R and/or WAIS-III was administered to 241 neurological patients who were being evaluated in connection with their enrollment in the Iowa Cognitive Neuroscience Patient Registry at the University of Iowa, over the course of more than a decade. Under the auspices

of the Registry, the patients had been extensively characterized in terms of their neuropsychological (Tranel, 2007) and neuroanatomical status (Frank et al., 1997). Demographic data are given in Table 1. Where multiple datasets were available, we chose neuropsychological and neuroanatomical datasets that were as contemporaneous as possible. All patients had single, focal, stable, chronic lesions of the brain, and we excluded those with progressive disease or psychiatric illness. All subjects had given written informed consent to participate in these research studies.

### Neuropsychological data

All subjects were tested individually on the WAIS-R or the WAIS-III (or both) by trained neuropsychologists in the Iowa Benton Neuropsychology Clinic. Index scores were based on the WAIS-III, and subjects who only had WAIS-R scores had their scores converted to WAIS-III equivalents according to the standardized scores reported in the WAIS-III manual. Scores for the four cognitive indices were calculated from these final scores by taking the mean of all the available and contributing subscales (see Supplemental Methods for full details). We performed 2 promax-rotated common factor analyses on the WAIS-III subscales (extracting 4 factors using principal axis factoring) in order to verify that these cognitive domains were preserved after brain damage. The first analysis (n=117) excluded 3 subtests (matrix reasoning, letter-number sequencing, and symbol search) which were undersampled compared to the rest, and a second analysis included only those patients with complete data sets (n=66). All factor analyses were carried out using SPSS (version 16). Replicability of the original loading matrix was statistically evaluated with the similarity index RV (Abdi, 2007).

### Neuroanatomical data

All neuroanatomical data were mapped using “MAP-3” as described previously (Damasio and Frank, 1992; Frank et al., 1997). Briefly, the visible lesion in each subject’s MRI or CT scan was manually traced, slice-by-slice, onto corresponding regions of a single, normal reference brain (template brain) that has been used in all prior studies with this method. All of the lesions were traced by a single expert (Hanna Damasio) who has demonstrated high reliability (Fiez et al., 2000). This manual tracing was only done when confidence could be achieved for matching corresponding slices between the lesion brain and the reference brain, and when confidence could be achieved for delineating the boundaries of the lesion accurately; thus lesions with unclear boundaries or lesions in brains whose mapping onto the reference brain was problematic were excluded (this excluded many subjects who only had CT scans and notably all subjects with metallic clips that produced artifacts on scans). Furthermore, as a quality assurance measure lesion traces were checked for consistency. Lesion volume was determined as the sum of all voxels comprising the traced lesion (in all slices) multiplied by the voxel volume ( $1 \text{ mm}^3$ ) after resampling.

### Lesion analysis

Because the neuroanatomical data was manually traced to a stereotaxic template, no automated spatial normalization was required. The lesion maps for each subject were resampled to an isotropic voxel size of  $1 \text{ mm}^3$ , spatially smoothed with a 4 mm full-width-at-half-maximum (FWHM) Gaussian kernel, binarized at a threshold of 0.2, and finally converted to the NiFTI file format. In order to facilitate the comparison with functional neuroimaging data we created a table of voxel coordinates of the peak lesion deficit relationship in the standard space Montreal Neurological Institute (MNI) (Table 3). We used Statistical Parametric Mapping (SPM5, <http://www.fil.ion.ucl.ac.uk/spm>) to coregister and normalize the Iowa template brain (Damasio, 2005) into MNI space (Evans et al., 1993). Regional labels were determined using the AAL templates (Tzourio-Mazoyer et al., 2002).

We performed a non-parametric voxel-based lesion symptom mapping (VLSM) analysis (Bates et al., 2003), which compared the neuropsychological scores between patients whose lesion either included or excluded a given voxel. We used the Brunner-Munzel (BM) test (Brunner and Munzel, 2000) at a threshold of 1% false discovery rate (FDR; corresponding to a critical Z-threshold of 3.1). This test is implemented in the “Nonparametric Mapping (NPM)” tool which is a part of the MRICron software package (Rorden et al., 2007) (<http://www.sph.sc.edu/comd/rorden/mricron/>). The BM test is a non-parametric implementation of a two-group comparison on a continuous variable which allows for heteroscedasticity of the variances between the groups (Brunner and Munzel, 2000). It is more appropriate than the t-test when the data are not normally distributed or when it is not obtained from an interval scale (Rorden et al., 2007). We placed an initial lower bound on statistical power by including in all subsequent analyses only those voxels having a lesion overlap from at least 4 patients.

Because VLSM analyses are particularly vulnerable to the multiple comparisons problem due to the univariate voxel-based nature of the analysis (the high spatial resolution of the scans means that hundreds of thousands of comparisons are computed), we controlled for false positives using a false discovery rate correction (FDR) (Nichols and Hayasaka, 2003). This procedure controls the ratio of false positives to hits, in contrast to methods for controlling the absolute false positive rate (as seen with familywise error correction techniques such as Bonferroni correction). FDR offers better statistical power than Bonferroni correction in situations where a substantial proportion of the tests include a discernable effect. We also applied a cluster extent threshold of  $k=100$  voxels, where a cluster was defined by voxels sharing a face (but not an edge or a corner).

### Statistical Power

In order to assess the specificity of our findings we computed power maps (Rudrauf et al., 2008a) that showed in which brain areas we had enough statistical power to detect a significant effect of brain lesion using the same threshold as our primary analysis. A novel aspect of the present study is the adaptation of these prospective lesion power maps to situations where the behavioral data is continuous rather than binomial. To achieve this, we used the Wilcoxon-Mann-Whitney probability as an estimate of power. For example if our population included ten patients and a given voxel was lesioned in three of these individuals, the most extreme ranking would be  $W=6$  (patients with lesions had the ranks of worst, second worst and third worst performance, and these ranks sum to six), with a resulting p-value of  $p<0.01667$ , corresponding to a Z score of 2.13. Therefore, if our statistical threshold was  $Z>3.1$ , we would not expect to be able to detect such a voxel, no matter how big the effect size.

### Sensitivity and Specificity

We conducted an ROC (receiver-operating characteristic) analysis to assess the reliability of the findings from the VLSM analysis (see Figure 2). In order to obtain an independent measure of how well each patient matched the findings of the entire sample, we conducted a leave-1-out VLSM analysis for each subject and calculated the overlap of each subject with the thresholded statistical map of the remaining group (without that particular subject) (BM test, 1% FDR). These leave-1-out analyses produced results highly consistent with the group analysis of all subjects (Figure 2) as they all shared more than 95% of the significant voxels (POI: 99%, ( $\pm 0.02$  S.D); PSI: 97% ( $\pm 0.03$  S.D); VCI: 99% ( $\pm 0.02$  S.D); WMI: 95% ( $\pm 0.03$  S.D)). We then used these overlap measures from all subjects in combination with their index scores to classify them according to the following confusion matrix:

		Lesion in ROI	
		Yes	No
Deficit	Yes	Hit	False Alarm
	No	Miss	Correct Rejection

A lesion was classified within the region of interest (ROI) if a patient's lesion overlap with the thresholded group map exceeded a certain percentage. Likewise, a patient was classified as having a deficit if his index score was below a certain cutoff. Based on the confusion matrix we computed the hit rate (HR) as  $\text{Hit}/(\text{Hit}+\text{Miss})$  and the false alarm rate (FAR) as  $\text{False Alarm}/(\text{False Alarm}+\text{Correct Rejection})$ . We varied the threshold for lesion overlap from 10% to 40%. Similarly, the cutoff for having a deficit was varied from the 20<sup>th</sup> to 80<sup>th</sup> percentile of the index score. For each of the overlap thresholds we computed the area under the ROC curve (AUC) by trapezoidal integration (Pollack and Hsieh, 1969) and averaged these AUC measures to obtain a representative performance measure for each index score. The AUC is a measure of how well (in terms of both sensitivity and specificity) the WAIS-III index score can predict a lesion in the brain regions defined by the VLSM analysis shown in Figure 2.

In order to assess whether these AUC were statistically significant, we chose a non-parametric permutation approach and created an empirical null distribution by 10000 random permutations of the index scores and lesion maps across all subjects and computed the AUC for each of them as described above. We chose the 99<sup>th</sup> percentile as the critical threshold. Sensitivity of the original assignment of index score to lesion maps of each index score was deemed significant if it exceeded this threshold (see Figure 5), thereby indicating that a deficit on that WAIS-III index is a sensitive predictor of a brain lesion in an area defined by the VLSM analysis.

We also assessed the specificity of each WAIS-III index by computing cross-validation AUC measures, i.e. using the data of one index score with the overlap measures of a different score. This is testing whether a deficit on an index score can also predict a lesion in a brain area *not* associated with that index scores, thereby indicating that it is not a predictor of specific brain damage. These cross-validation AUCs for each index score were then also compared against the empirical null distribution of the other index score (e.g. when using VCI to predict the overlap pattern found with POI, the resulting AUC was compared against the null distribution of POI). These cross-validation AUCs are also shown in Figure 5.

## Supplementary Material

Refer to Web version on PubMed Central for supplementary material.

## Acknowledgments

Supported in part by the Akademie der Naturforscher Leopoldina LPD Grant 9901/8–140 (JG), by grants from the National Institutes of Health: R01 NS054266 (CR), P01 NS19632 (DT, HD, RA) and R01 DA022549 (DT), and by the Gordon and Betty Moore Foundation (RA). The authors declare no conflict of interest.

## References

- Abdi, H. RV coefficient and congruence coefficient. In *Encyclopedia of Measurement and Statistics*. Salkind, N., editor. Thousand Oak, CA: Sage; 2007.
- Adolphs R, Damasio H, Tranel D, Cooper G, Damasio AR. A role for somatosensory cortices in the visual recognition of emotion as revealed by three-dimensional lesion mapping. *J Neurosci* 2000;20:2683–2690. [PubMed: 10729349]
- Bar-On R, Tranel D, Denburg NL, Bechara A. Exploring the neurological substrate of emotional and social intelligence. *Brain* 2003;126:1790–1800. [PubMed: 12805102]
- Bates E, Wilson SM, Saygin AP, Dick F, Sereno MI, Knight RT, Dronkers NF. Voxel-based lesion-symptom mapping. *Nat Neurosci* 2003;6:448–450. [PubMed: 12704393]

- Bornstein RA, Matarazzo JD. Wechsler VIQ versus PIQ differences in cerebral dysfunction: a literature review with emphasis on sex differences. *J Clin Neuropsychol* 1982;4:319–334. [PubMed: 6757270]
- Broca PP. Remarques sur le siège de la faculté de langage articulé, suivies d'une observation d'aphémie (perte de la parole). *Bulletin de la Societe de Anatomie* 1861;36
- Brunner E, Munzel U. The Nonparametric Behrens-Fisher Problem: Asymptotic Theory and a Small-Sample Approxiamtion. *Biometrical Journal* 2000;42:17–25.
- Colom R, Jung RE, Haier RJ. Distributed brain sites for the g-factor of intelligence. *Neuroimage* 2006a; 31:1359–1365. [PubMed: 16513370]
- Colom R, Jung RE, Haier RJ. Finding the g-factor in brain structure using the method of correlated vectors. *Intelligence* 2006b;34:561–570.
- Damasio, H. *Human Brain Anatomy in Computerized images*. Vol. 2. New York: Oxford University Press; 2005.
- Damasio H, Frank R. Three-dimensional in vivo mapping of brain lesions in humans. *Arch Neurol* 1992;49:137–143. [PubMed: 1736845]
- Damasio H, Grabowski T, Frank R, Galaburda AM, Damasio AR. The return of Phineas Gage: clues about the brain from the skull of a famous patient. *Science* 1994;264:1102–1105. [PubMed: 8178168]
- Damasio H, Tranel D, Grabowski T, Adolphs R, Damasio A. Neural systems behind word and concept retrieval. *Cognition* 2004;92:179–229. [PubMed: 15037130]
- DeLuca J, Chelune GJ, Tulsy DS, Lengenfelder J, Chiaravalloti ND. Is speed of processing or working memory the primary information processing deficit in multiple sclerosis? *J Clin Exp Neuropsychol* 2004;26:550–562. [PubMed: 15512942]
- Dronkers NF, Wilkins DP, Van Valin RD Jr, Redfern BB, Jaeger JJ. Lesion analysis of the brain areas involved in language comprehension. *Cognition* 2004;92:145–177. [PubMed: 15037129]
- Duncan J, Seitz RJ, Kolodny J, Bor D, Herzog H, Ahmed A, Newell FN, Emslie H. A neural basis for general intelligence. *Science* 2000;289:457–460. [PubMed: 10903207]
- Evans AC, Collins DL, Mills DR, Brown ED, Kelly RL, Peters TM. 3D statistical neuroanatomical model from 205 MRI volumes. *Proc IEEE Nucl Sci Symp Med Imaging* 1993;1:1813–1817.
- Fiez JA, Damasio H, Grabowski TJ. Lesion segmentation and manual warping to a reference brain: intra- and interobserver reliability. *Hum Brain Mapp* 2000;9:192–211. [PubMed: 10770229]
- Fisher DC, Ledbetter MF, Cohen NJ, Marmor D, Tulsy DS. WAIS-III and WMS-III profiles of mildly to severely brain-injured patients. *Appl Neuropsychol* 2000;7:126–132. [PubMed: 11125705]
- Frank RJ, Damasio H, Grabowski TJ. Brainvox: an interactive, multimodal visualization and analysis system for neuroanatomical imaging. *Neuroimage* 1997;5:13–30. [PubMed: 9038281]
- Gray JR, Chabris CF, Braver TS. Neural mechanisms of general fluid intelligence. *Nat Neurosci* 2003;6:316–322. [PubMed: 12592404]
- Haier RJ, Jung RE, Yeo RA, Head K, Alkire MT. Structural brain variation and general intelligence. *Neuroimage* 2004;23:425–433. [PubMed: 15325390]
- Haier RJ, Jung RE, Yeo RA, Head K, Alkire MT. The neuroanatomy of general intelligence: sex matters. *Neuroimage* 2005;25:320–327. [PubMed: 15734366]
- Harlow JM. Passage of an iron rod through the head. *Boston Med Surg Journal* 1848;39
- Jensen, AR. *The g factor: The science of general intelligence*. Praeger; 1998.
- Jung RE, Haier RJ. The Parieto-Frontal Integration Theory (P-FIT) of intelligence: converging neuroimaging evidence. *Behav Brain Sci* 2007;30:135–154. [PubMed: 17655784]discussion 154–187
- Jung RE, Haier RJ, Yeo RA, Rowland LM, Petropoulos H, Levine AS, Sibbitt WL, Brooks WM. Sex differences in N-acetylaspartate correlates of general intelligence: an 1H-MRS study of normal human brain. *Neuroimage* 2005;26:965–972. [PubMed: 15955507]
- Karnath HO, Ferber S, Himmelbach M. Spatial awareness is a function of the temporal not the posterior parietal lobe. *Nature* 2001;411:950–953. [PubMed: 11418859]
- Kennedy JE, Clement PF, Curtiss G. WAIS-III processing speed index scores after TBI: the influence of working memory, psychomotor speed and perceptual processing. *Clin Neuropsychol* 2003;17:303–307. [PubMed: 14704894]

- Kido DK, Cox C, Hamill RW, Rothenberg BM, Woolf PD. Traumatic brain injuries: predictive usefulness of CT. *Radiology* 1992;182:777–781. [PubMed: 1535893]
- Levine B, Black SE, Cheung G, Campbell A, O'Toole C, Schwartz ML. Gambling task performance in traumatic brain injury: relationships to injury severity, atrophy, lesion location, and cognitive and psychosocial outcome. *Cogn Behav Neurol* 2005;18:45–54. [PubMed: 15761276]
- Nichols T, Hayasaka S. Controlling the familywise error rate in functional neuroimaging: a comparative review. *Stat Methods Med Res* 2003;12:419–446. [PubMed: 14599004]
- Owen AM, McMillan KM, Laird AR, Bullmore E. N-back working memory paradigm: a meta-analysis of normative functional neuroimaging studies. *Hum Brain Mapp* 2005;25:46–59. [PubMed: 15846822]
- Pollack I, Hsieh R. Sampling variability of the areas under the ROC-curve and of  $d'$ . *Psychol Bull* 1969;71:161–173.
- Price CJ, Friston KJ. Degeneracy and cognitive anatomy. *Trends Cogn Sci* 2002;6:416–421. [PubMed: 12413574]
- Price CJ, Mummery CJ, Moore CJ, Frakowiak RS, Friston K. Delineating necessary and sufficient with functional neuroimaging studies of neuropsychological patients. *J Cogn Neurosci* 1999;11:371–381. [PubMed: 10471846]
- Rafal RD. Oculomotor function of the parietal lobe: effects of chronic lesions in humans. *Cortex* 2006;42:730–739. [PubMed: 16909633]
- Ringo JL, Doty RW, Demeter S, Simard PY. Time is of the essence: a conjecture that hemispheric specialization arises from interhemispheric conduction delay. *Cereb Cortex* 1994;4:331–343. [PubMed: 7950307]
- Rorden C, Karnath HO, Bonilha L. Improving lesion-symptom mapping. *J Cogn Neurosci* 2007;19:1081–1088. [PubMed: 17583985]
- Rubin LA, Barr WB, Burton LA. Assessment practices of clinical neuropsychologists in the United States and Canada: A survey of INS, NAN, and PAP Division 40 members. *Arch Clin Neuropsychol* 2005;20:33–65. [PubMed: 15620813]
- Rudrauf D, Mehta S, Bruss J, Tranel D, Damasio H, Grabowski TJ. Thresholding lesion overlap difference maps: application to category-related naming and recognition deficits. *Neuroimage* 2008a;41:970–984. [PubMed: 18442925]
- Rudrauf D, Mehta S, Grabowski TJ. Disconnection's renaissance takes shape: Formal incorporation in group-level lesion studies. *Cortex* 2008b;44:1084–1096. [PubMed: 18625495]
- Ryan JD, Cohen NJ. Evaluating the neuropsychological dissociation evidence or multiple memory systems. *Cogn Affect Behav Neurosci* 2003;3:168–185. [PubMed: 14672154]
- Scoville WB, Milner B. Loss of recent memory after bilateral hippocampal lesions. *J Neurol Neurosurg Psychiatry* 1957;20:11–21. [PubMed: 13406589]
- Smith EE, Jonides J. Neuroimaging analyses of human working memory. *Proc Natl Acad Sci U S A* 1998;95:12061–12068. [PubMed: 9751790]
- Sternberg RJ. Cognition. The holy grail of general intelligence. *Science* 2000;289:399–401. [PubMed: 10939950]
- The Psychological Corporation. WAIS-III/WMS-III Technical Manual. San Antonio, TX: Author; 1997.
- Tranel, D. Theories of clinical neuropsychology and brain-behavior relationships: Luria and beyond. In: Morgan, JE.; Ricker, JH., editors. *Testbook of clinical neuropsychology*. New York: Taylor and Francis; 2007. p. 27-37.
- Tulsky, DS.; Ivnik, RJ.; Price, LR.; Wilkins, C. Assessment of cognitive functioning with the WAIS-III and WMS-III: Development of a 6-factor model. In: Tulsky, DS.; Saklofske, GJ.; Chelune, GJ.; Heaton, RK.; Ivnik, RJ.; Bornstein, RA., editors. *Clinical Interpretation of the WAIS-III and WMS-III*. San Diego, CA: Academic Press; 2003. p. 147-179.
- Tulsky DS, Price LR. The joint WAIS-III and WMS-III factor structure: development and cross-validation of a six-factor model of cognitive functioning. *Psychol Assess* 2003;15:149–162. [PubMed: 12847775]
- Turken A, Whitfield-Gabrieli S, Bammer R, Baldo JV, Dronkers NF, Gabrieli JD. Cognitive processing speed and the structure of white matter pathways: convergent evidence from normal variation and lesion studies. *Neuroimage* 2008;42:1032–1044. [PubMed: 18602840]

- Tzourio-Mazoyer N, Landeau B, Papathanassiou D, Crivello F, Etard O, Delcroix N, Mazoyer B, Joliot M. Automated anatomical labeling of activations in SPM using a macroscopic anatomical parcellation of the MNI MRI single-subject brain. *Neuroimage* 2002;15:273–289. [PubMed: 11771995]
- Ungerleider LG, Haxby J. What and Where in the Human Brain. *Curr Opin Neurobiol* 1994;4:159–160.
- van der Heijden P, Donders J. WAIS-III factor indexscore patterns after traumatic brain injury. *Assessment* 2003;10:115–122. [PubMed: 12801182]
- Warrington EK, James M, Maciejewski C. The WAIS as a lateralizing and localizing diagnostic instrument: a study of 656 patients with unilateral cerebral lesions. *Neuropsychologia* 1986;24:223–239. [PubMed: 3714027]
- Wechsler, D. Wechsler Adult Intelligence Scale. New York: The Psychological Corporation; 1955.
- Wechsler, D. Wechsler Adult Intelligence Scale-Revised. San Antonio, TX: The Psychological Corporation; 1981.
- Wechsler, D. Wechsler Adult Intelligence Scale . Vol. 3. San Antonio, TX: The Psychological Corporation; 1997.
- Zhu J, Tulskey DS, Price L, Chen HY. WAIS-III reliability data for clinical groups. *J Int Neuropsychol Soc* 2001;7:862–866. [PubMed: 11771629]

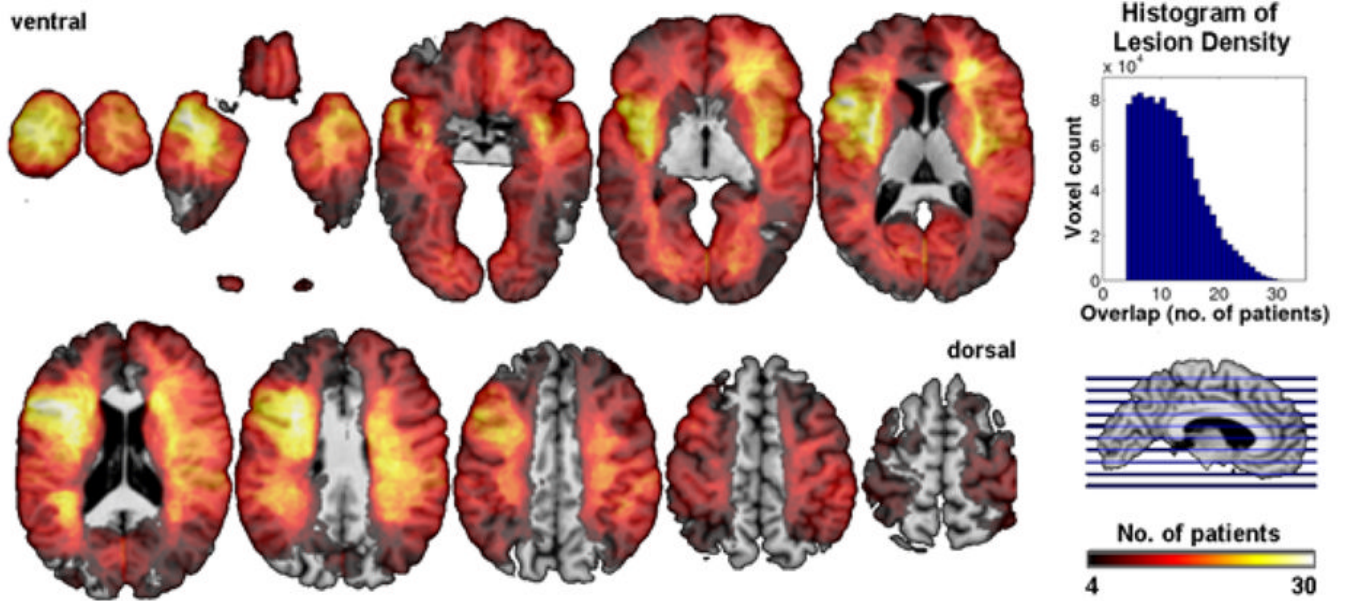


**Figure 1.** Lesion density overlap map for all 241 patients. We restricted all analyses to a minimum overlap of 4 patients in a given voxel. The maximum overlap of 33 patients occurred in the left inferior frontal cortex. Horizontal cuts encode lesion overlap density by color.



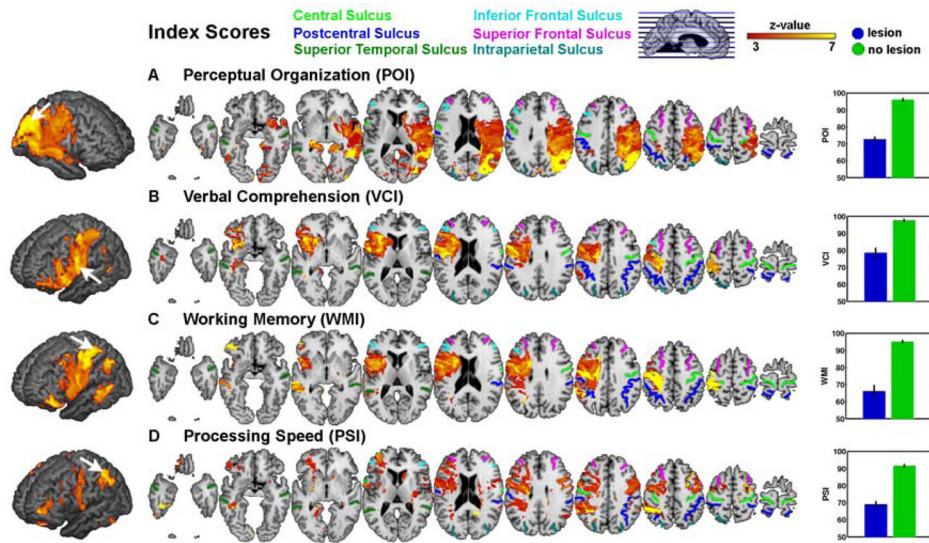


**Figure 2.**

Voxel-based lesion symptom mapping of four cognitive indices of intelligence. Our VLSM analyses compared the index scores for patients with a lesion against those without a lesion, at each and every voxel. All colored regions in the slice-wise display and the 3D projection (left; search depth 8 mm) survived a statistical threshold of 1% FDR. The size of the effect (greater Z-values) is color-coded with warmer colors corresponding to a greater difference. The graphs on the right show the mean difference on each index score between those patients whose lesions included the voxel showing the maximum effect (black arrow on the 3D projection) and those whose lesions did not include it (errorbar = s.e.m.). (a) perceptual organization (b) verbal comprehension, (c) working memory, (d) processing speed.

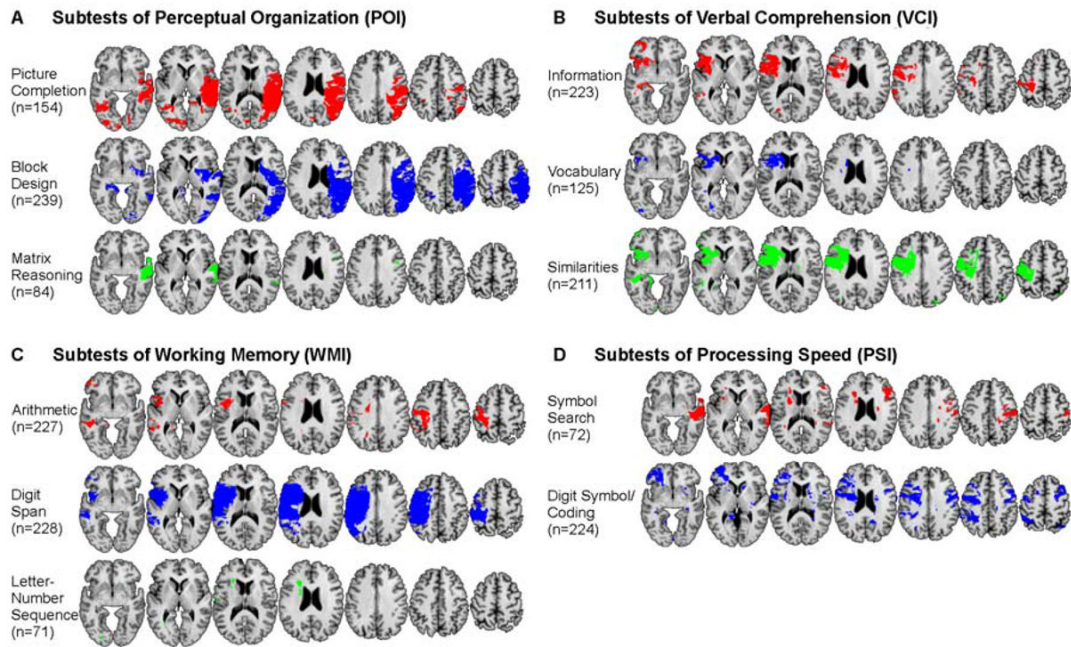


**Figure 3.** VLSM analyses for all subtests from the Wechsler Adult Intelligence Scale. Subtests are grouped within the same four cognitive indices shown in Figure 2, and with the same uniform statistical thresholds as in Figure 2 (1% FDR). Regions with significant lesion-deficit relationships are thresholded and shown in unique colors corresponding to each subtest.

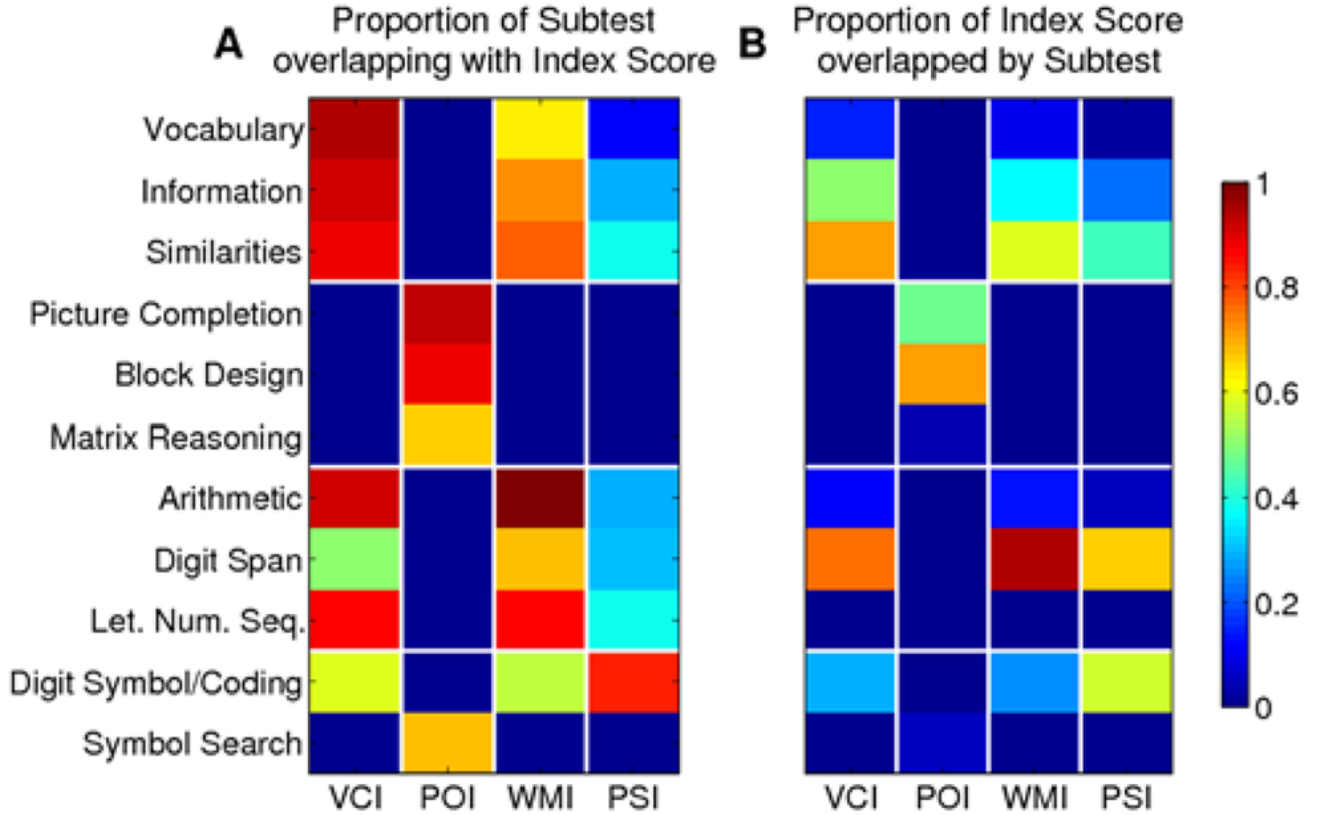


**Figure 4.**

Overlap of subtests with index scores. (A) Proportion of significant voxels of each subtest that overlap with each index score as calculated by  $N_{OVLP}/N_{ST}$  ( $N_{OVLP}$  = number of significant voxels in overlap,  $N_{ST}$  = number of significant voxels in subtest). (B) Proportion of significant voxels in index that are overlapped by each subtest as calculated by  $N_{OVLP}/N_I$  ( $N_I$  = number of significant voxels for index score).

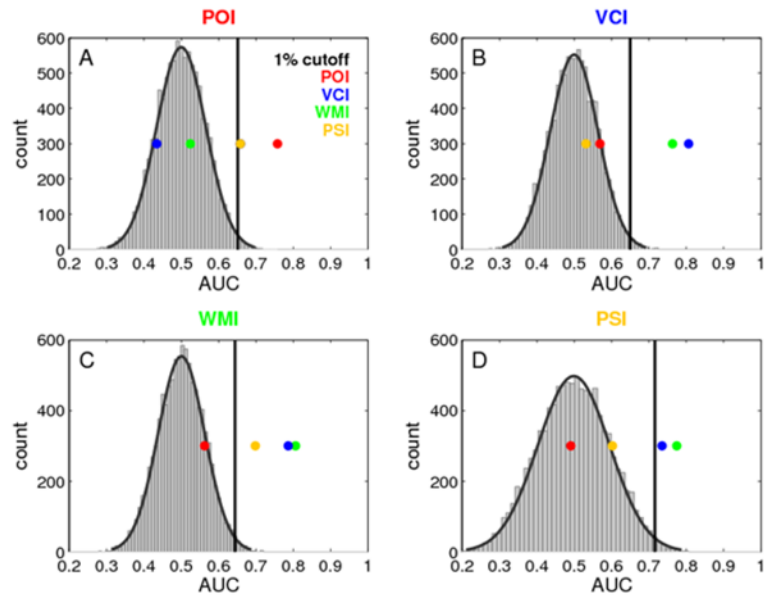


**Figure 5.** Specificity and sensitivity of the findings. Area under the ROC curve (AUC) is shown for each index score in a cross-validation analysis (four colored dots). The ROC was derived from each index score and an independent overlap measure for each patient with the rest of the sample in individual leave-one-out VLSM analyses. The empirical null distribution (gray histogram with Gaussian fit superimposed) was derived by 10000 permutations of the index scores. The 99th percentile of this distribution was defined as the critical threshold for statistical significance. The colored dots indicate the AUC of the original ordering of index scores and overlap measures (the colored dot that corresponds to the title of each graph) (sensitivity) as well as the AUC of each other index score with the individual overlap measure (specificity).

**Table 1**  
Demographics, lesion volume, and etiology for 241 lesion patients.

<b>Etiology</b>	<b>N</b>	<b>Age (sd)</b>	<b>Gender (f/m)</b>	<b>Edu. (yrs)</b>	<b>Volume (ml) (sd)</b>	<b>Hand (l/r)</b>
Cerebrovascular Disease	188	52.4 (14.2)	85/103	12.7	57.5 (63.3)	20/168
Anterior Temporal Lobectomy	30	32.0 (10.3)	16/14	13.5	43.5 (17.2)	4/26
Surgical Intervention	16	45.6 (14.4)	6/10	13.3	67.9 (53.6)	0/16
Herpes Simplex Encephalitis	3	38.0 (25.4)	2/1	13.8	127.2 (6.8)	0/3
Traumatic Brain Injury	4	21.3 (5.5)	1/3	11.0	33.4 (17.6)	0/4
Overall	241	48.8 (15.8)	110/131	12.8	56.9 (58.6)	24/217

**Table 2**

## WAIS-III subtests and index scores

Index Score	Subtest
POI	Block Design
	Picture Completion
	Matrix Reasoning
VCI	Vocabulary
	Similarities
	Information
WMI	Digit Span
	Arithmetic
	Letter-Number Sequence
PSI	Digit Symbol/Coding
	Symbol Search
	<i>additional subtests not belonging to any index score:</i>
	Object assembly
	Picture Arrangement
	Comprehension

Table 3

MNI coordinates and Z-score of peak lesion deficit relationship for WAIS index scores. The Iowa template brain used in the figures was coregistered and normalized into MNI space (Evans et al., 1993) using Statistical Parametric Mapping (SPM). Region labels are taken from the AAL template (Tzourio-Mazoyer et al., 2002). Z-scores are derived from computing p-values from the Brunner-Munzel test statistic and then converting the p-value to a Z-score using a normal distribution.

Index Score	Region	Hemi	x	y	z	Z	
POI	Temporal Mid	R	44	-54	20	6.51	
	Temporal Sup	R	52	-12	4	6.64	
	Temporal Sup	R	62	-40	22	6.99	
	Angular	R	54	-50	36	6.95	
	Parietal Inf	R	56	-50	48	6.42	
	Parietal Inf	R	34	-40	48	6.71	
	Postcentral	R	40	-16	38	6.34	
	Occipital Mid	R	32	-76	28	6.38	
	Frontal Inf Tri	L	-30	8	16	6.91	
	Insula	L	-38	19	4	6.96	
VCI	Rolandic Operculum	L	-40	24	4	6.92	
	Frontal Inf Operculum	L	-36	10	-2	6.78	
	Precentral	L	-50	-2	20	6.67	
	Precentral	L	-50	0	30	7.08	
	Putamen	L	-28	1	13	6.88	
	Postcentral	L	-30	-32	50	6.43	
	Temporal Mid	L	-60	-38	0	6.24	
	Precentral	L	-52	0	22	6.83	
	Postcentral	L	-24	40	50	6.95	
	Rolandic Operculum	L	-42	0	16	6.10	
PSI	Angular	L	-42	-60	38	6.78	
	Frontal Mid	R	30	2	52	6.64	
	Precentral	L	-34	-10	50	5.32	
	Postcentral	R	56	-2	32	5.38	
	Parietal Inf	L	-42	-44	54	6.94	
	Parietal Inf	L	-58	-52	44	6.10	
	Lingual	L	-20	-46	0	6.46	